

1
2
3
4
5
6
7
8
9
10
11
12
13
14
15
16
17
18
19
20
21
22
23
24
25
26

Time-resolved compound repositioning predictions on a texted-mined knowledge network

Michael Mayers, Tong Shu Li, Núria Queralt-Rosinach, Andrew I Su.

The Scripps Research Institute, 10550 N Torrey Pines Rd. La Jolla, CA 92037, USA.

mmayers@scripps.edu, tongli@scripps.edu, nuriaqr@scripps.edu, asu@scripps.edu

27 **Abstract**

28 **Background**

29 Computational compound repositioning has the potential for identifying new uses for existing drugs, and
30 new algorithms and data source aggregation strategies provide ever-improving results via *in silico*
31 metrics. However, even with these advances, the number of compounds successfully repositioned via
32 computational screening remains low. New strategies for algorithm evaluation that more accurately
33 reflect the repositioning potential of a compound could provide a better target for future optimizations.

34 **Results**

35 Using a text-mined database, we applied a previously described network-based computational
36 repositioning algorithm, yielding strong results via cross-validation, averaging 0.95 AUROC on test-set
37 indications. The text-mined data was then used to build networks corresponding to different time-points
38 in biomedical knowledge. Training the algorithm on contemporary indications and testing on future
39 showed a marked reduction in performance, peaking in performance metrics with the 1985 network at an
40 AUROC of .797. Examining performance reductions due to removal of specific types of relationships
41 highlighted the importance of drug-drug and disease-disease similarity metrics. Using data from future
42 timepoints, we demonstrate that further acquisition of these kinds of data may help improve
43 computational results.

44 **Conclusions**

45 Evaluating a repositioning algorithm using indications unknown to input network better tunes its ability to
46 find emerging drug indications, rather than finding those which have been withheld. Focusing efforts on
47 improving algorithmic performance in a time-resolved paradigm may further improve computational
48 repositioning predictions.

49

50 **Keywords**

51 Heterogeneous Network, Semantic Medline Database, Semantic Network, Unified Medical Language
52 System, Drug Central, Compound Repositioning, Machine Learning

53

54 **Background**

55 Compound repositioning is the identification and development of new uses for previously existing drugs.
56 Repositioning is an attractive pipeline for drug development primarily due to the reduced pharmaceutical
57 uncertainty and development times when compared to traditional pipelines [1]. While clinical observation
58 and improved understanding of the mechanism of action are the two primary means by which a drug is
59 repositioned, computational repositioning provides a third route to identifying these candidates. This third
60 method has seen much development in the past decade as a way to potentially speed up the drug
61 discovery process. The ultimate goal of computational repositioning is to quickly produce a small number
62 of clinically relevant hits for further investigation. This process is achieved through the identification of
63 features that relate drugs to diseases and utilizes a gold standard of known true drug-treats-disease
64 relationships to train an algorithm to categorize or rank potential drug-disease pairs for treatment
65 probability. While this path can efficiently produce repositioning probabilities for countless drug-disease
66 pairs, identifying and experimentally validating the results of clinical importance can be both costly and
67 challenging [2].

68 In the last decade, there have been many improvements in approaches and algorithms to identify
69 these candidates [3]. These include an expansion from gene expression-based approaches [4, 5] to include
70 methods based on knowledge graphs [6, 7]. Coupled with the advancements in machine learning, the
71 number of different methods for producing repurposing predictions has quickly increased, each showing
72 marked improvements on their ability to accurately predict candidates. One common result in these
73 knowledge-based approaches is that drug-drug and disease-disease similarity, when combined with drug-
74 disease associations, provide the important information for generating a learning model [6, 8, 9]. Many
75 different metrics can be used to express these similarities, like structural motifs in the case of drugs, or
76 phenotypes in the case of diseases. However, as good as these algorithms have become at providing
77 repurposing candidates from a list of known indications, the majority of computational repositioning
78 projects do not continue beyond the *in vitro* studies [10].

79 One recent effort in computational repositioning, Himmelstein et. al.'s Rephetio project [11] used
80 a heterogeneous network (hetnet) to describe drug-disease relationships in a variety of ways. This method
81 worked by extracting counts of various metapaths between drug-disease pairs, where a metapath is
82 defined by the concept and relationship types in the knowledge graph that join the drug and disease.
83 These metapaths counts are then used as numerical features in a machine learning model. This study
84 compiled several different highly curated data sources to generate the hetnet underlying this learning
85 model and achieved excellent performance results. Whether this learning model that utilizes network
86 structure as features can achieve similar results with a less well-curated network remains an open
87 question.

88 Progress in the field of natural language processing (NLP) has led to the ability to generate large
89 biomedical knowledge bases through computational text-mining [12, 13]. This method can produce large
90 amounts of data rather quickly, which when coupled with semantic typing of concepts and relations,
91 produces a massive datasource that can quickly be represented in a hetnet structure.

92 In this work, we evaluated the utility of text-mined networks for use in computational compound
93 repositioning, by utilizing the Semantic MEDLINE Database (SemMedDB) [14] as an NLP-derived
94 knowledge network, and the Rephetio algorithm for producing predictions. We evaluated the
95 performance of this data source when trained with a gold standard of indications taken from DrugCentral
96 [15] and tested via cross-validation. We then propose a new framework for evaluating repurposing
97 algorithms in a time-dependent manner. By utilizing one of the unique features of SemMedDB, a PubMed
98 Identification number (PMID) documented for every edge in the network, multiple networks were
99 produced in a time-resolved fashion, each with data originating on or before a certain date, representing
100 the current state of knowledge at that date. These networks were then evaluated in the context of
101 computational repositioning via training on indications known during the time period of the given
102 network and tested on indications approved after the network, a paradigm that more closely resembles the
103 real-world problem addressed by computational repositioning than a cross-validation. Finally, we
104 analyzed these results to identify the types of data most important to producing accurate predictions and

105 tested the predictive utility of supplementing a past network with future knowledge of these important
106 types.

107

108 **Methods**

109 **Initial SemMedDB Network Generation**

110 The SemMedDB SQL dump Version 31R, processed through June 30, 2018, was downloaded
111 (<https://skr3.nlm.nih.gov/SemMedDB/download/download.html>) and converted into a csv. Using Python
112 scripts (<https://github.com/mmayers12/semmed/tree/master/prepare>), corrupted lines were removed, and
113 lines were normalized to a single subject-predicate-object triple per line, with identifiers in Unified
114 Medical Language System (UMLS) space. This ‘clean’ database was then further processed into a
115 heterogeneous network (hetnet) compatible with the hetnet package, hetio (<https://github.com/hetio/hetio>)
116 a prerequisite for the rephetio machine learning pipeline. This processing included: using the UMLS
117 Metathesaurus version 2018AA to map terms to other identifier spaces (primarily Medical Subject
118 Headings or MeSH), combining granular concepts into a more general terms, thus reducing node-count
119 and data-redundancy; combining semantic (edge) types of similar meaning (e.g. between Chemicals &
120 Drugs and Disorders, ‘TREATS’, ‘PREVENTS’, ‘DISRUPTS’, and ‘INHIBITS’ were merged to
121 ‘TREATS’); filtering out semantic edge types that were sparsely populated (less than 0.1% of the total
122 network); removing the top 100 nodes by degree to eliminate extremely general concepts (e.g., Patients,
123 Cells, Disease, Humans); filtering out edges with less than 2 supporting PMIDs to reduce data noise due
124 to text-mining.

125 To create time-resolved knowledge networks, a map between PMID and publication year was
126 generated from four data sources: Pubmed Central (<ftp://ftp.ncbi.nlm.nih.gov/pub/pmc/>), Euro PMC
127 (<http://europepmc.org/ftp/pmclitemetadata/>), NLM - Baseline Repository
128 (<ftp://ftp.ncbi.nlm.nih.gov/pubmed/baseline/>), and EBI’s API (<https://europepmc.org/RestfulWebService>).
129 Output from these sources was merged to encompass the greatest number of PMIDs possible. Networks

130 were generated at 5-year intervals starting at the year 1950 continuing to present day. The PMID with the
131 earliest publication year for a given edge was used for that edge.

132 **Gold standard generation**

133 The PostgreSQL dump of DrugCentral dated 2018-06-21 was downloaded for use as the gold standard of
134 known drug-disease indications. The following tables were extracted for use throughout the analysis
135 pipeline: *omap_relationship*, containing the indications; *identifier*, with maps from internal IDs to other
136 systems including UMLS and MeSH; *approval*, containing approval dates from worldwide medical
137 agencies; *synonyms*, containing drug names. Both DrugCentral's and UMLS's cross-references to MeSH
138 were used to map DrugCentral internal structure IDs to SemMedDB, ensuring maximum overlap. Disease
139 concepts contained both MeSH and Systematized Nomenclature of Medicine (SNOMED) identifiers that
140 could be mapped to SemMedDB via UMLS cross-references. Some diseases could not be mapped to
141 UMLS, primarily due to the specific nature of the condition, and were discarded. Unmappable conditions
142 included 'Uremic Bleeding Tendency', 'Tonic-Clonic Epilepsy Treatment Adjunct', and 'Prevention of
143 Stress Ulcer.' Highly related diseases were merged to produce a more general disease concept for each
144 treated disease. For example, 'Vasomotor rhinitis,' 'Allergic rhinitis', 'Perennial allergic rhinitis', and
145 'Seasonal allergic rhinitis,' were merged to the single concept 'Allergic rhinitis.' For time-resolved
146 analysis, the first approval year for a drug in an indication, provided by DrugCentral, was taken as a
147 proxy for the date of the indication.

148 **Repurposing Algorithm**

149 A customized version of the PathPredict algorithm [16] utilized in the Repehtio repurposing project [11]
150 was adapted for producing repurposing predictions on the SemMedDB hetnet. This algorithm utilizes
151 Degree Weighted Path Counts (DWPC) as the primary feature for machine learning [17]. These features
152 are based on the various metapaths that connect the source and target node types (in this case Chemicals
153 & Drugs, and Disorders). To aid in the speed of feature extraction, we built a framework
154 (https://github.com/mmayers12/hetnet_ml) based on multiplication of Degree-Weighted adjacency
155 matrices to extract path-counts quickly. The extracted features were then scaled and standardized

156 according to the Repheto framework. Finally, an ElasticNet regularized logistic regression was
157 performed using the python wrapper (<https://github.com/civisanalytics/python-glmnet>) for the Fortran
158 library used in the R package glmnet [18]. Hyperparameters were tuned via grid search and once chosen
159 left constant throughout all future runs.

160 To evaluate the model, the DrugCentral gold standard was partitioned by indication into 5 equal
161 partitions. One-fifth of the indications were withheld during training, and negative training examples were
162 sampled at a rate of ten times the number of positives from the set of non-positive drug-disease pairs. The
163 corresponding TREATS edges for holdout indications were removed from the hetnet before feature
164 extraction in an attempt to limit the model's ability to learn directly from those edges. The five-fold cross-
165 validations were performed a total of ten times, each with a different random partitioning.

166 **Time-restricted learning models**

167 The models for the time-resolved networks were trained using the positive gold-standard indications
168 where drug was approved in the years prior to and including the year of the network. Training negatives
169 were selected randomly from the pool of non-positive drug-disease pairs at a rate of ten times the number
170 of positives. After training, the models were then tested on positive indications dated after the year of the
171 network, as well as a proportional number of negatives.

172 To combine the results of all of the models across the varying network years, the prediction
173 probability for each model was first converted to z-score. This allowed for a cross model comparison of
174 the results. The standardized probabilities for gold-standard drug-disease indications were then grouped
175 according to the difference in years between the network the probability was derived from and the
176 approval year of the drug in the indication. This grouping allowed for the generation of performance
177 metrics for a relative drug approval year. Negative examples were chosen at random from the non-
178 positive set of drug-disease pairs, across all models, at a rate of ten times that of the positives. Area under
179 the receiver operator characteristic (AUROC) and precision recall curves (AUPRC) were then calculated
180 for each of the different time differences from negative 20 to positive 20 years.

181 **Feature performance analyses**

182 To test the relative importance of each edge type to the model, one of the better performing networks on
183 future indications, 1985, was chosen as a baseline. We performed a 'dropout' analysis in which edge
184 instances were removed randomly from the network at rates of 25%, 50%, 75%, and 100% before running
185 the machine learning pipeline. For dropout rates of 25%, 50%, and 75%, the 5 replicates were run with
186 different random seeds, to account for the differences that specific edges may produce when selected for
187 dropout. Performance metrics AUROC and AUPRC of these different dropout results were then
188 compared to the baseline 1985 network model result.

189 For the edge replacement analysis, the 1985 network was taken as a baseline. Edge instances of a
190 given type were, type by type, replaced with those from the networks of other years starting with 1950
191 and continuing to present. This produced 15 models for each of the 30 edge types, one for each network
192 year per edge type. For example, for the TREATS edge, all values from the 1985 network were removed
193 and replaced with TREATS edges from the 1950 network and predictions were made, then the TREATS
194 edges were replaced with those from the 1955 network, and so-forth. AUROC and AUPRC results from
195 these modified networks were compared to that of the base 1985 network.

196

197 **Results**

198 **5-fold cross-validation on text-mined data**

199 A hetnet comprised of biomedical knowledge was built from SemMedDB, a database containing subject,
200 predicate, object triples that were text-mined from PubMed abstracts. After data processing steps (see
201 methods) the final network contained 78,400 unique concepts (graph nodes) and 2,470,050 relations
202 (edges) connecting those concepts. These concepts were classified into 6 different types derived from
203 UMLS semantic groups – 'Chemicals & Drugs', 'Disorders', 'Genes & Molecular Sequences',
204 'Anatomy', 'Physiology', and 'Phenomena'. The relationships between the nodes were also classified as
205 one of 30 different edge types, comprised of both a semantic relation and the source and target node
206 types. For example, the relation 'AFFECTS' between nodes of type 'Chemicals & Drugs' and 'Anatomy'
207 is distinct from the relationship 'AFFECTS' between nodes of type 'Chemicals & Drugs' and

208 ‘Physiology’. In labeling these relations, the node abbreviations are appended to the semantic relation to
209 explicitly differentiate the edge types, e.g. the above examples the labels are ‘AFFECTS_CDafA’ and
210 ‘AFFECTS_CDafPH’ respectively (Table 1, and Supplemental Figure S1, Additional File 1). To train a
211 learning model for compound repurposing, a gold standard of high quality and reliability containing drug-
212 disease indications is required. We used DrugCentral as the source for our gold standard. This open drug
213 database contains a relatively complete, curated list of known indications, with a total of 10,938 unique
214 drug-disease pairs. In mapping these drug and disease concepts to those found in SemMedDB, 3,885
215 indications were lost due an inability to map the disease condition to a unique concept ID (see methods
216 for examples), and further reductions came due to the merging of highly related disease concepts,
217 resulting in 5,337 unique indications that could be used as true-positives for training and testing purposes.

218 Table 1: Top 10 Edge Types by Instance Number

Subject Node Type	Predicate	Object Node Type	Edge Abbreviation	Count
Anatomy	LOCATION_OF	Chemicals & Drugs	AloCD	380,422
Chemicals & Drugs	REGULATES	Chemicals & Drugs	CDreg>CD	214,912
Chemicals & Drugs	INTERACTS_WITH	Genes & Molecular Sequences	CDiwG	183,016
Anatomy	LOCATION_OF	Disorders	AloDO	182,373
Anatomy	LOCATION_OF	Genes & Molecular Sequences	AloG	174,246
Chemicals & Drugs	TREATS	Disorders	CDtDO	172,384
Disorders	ASSOCIATED_WITH	Disorders	DOawDO	169,075
Anatomy	LOCATION_OF	Anatomy	AloA	98,472
Chemicals & Drugs	STIMULATES	Genes & Molecular Sequences	CDstG	93,343
Chemicals & Drugs	AFFECTS	Anatomy	CDafA	92,126

219 After preparation of the hetnet and the gold standard, the utility of this text-mined knowledge
220 base for the prediction of novel drug-disease indications was examined using a modified version of the
221 PathPredict algorithm, utilized by Himmelstein et. al. in the Rephetio drug repurposing project [11]. This
222 paradigm utilizes the degree weighted path count (DWPC) metric, derived from the metapaths that

223 connect different concepts within a network, as the primary features for training the classifier [17]. The
224 remaining features, while comparatively small, are derived from the simple degree values of each edge
225 type for the drug node and the disease node in given drug-disease pair. A 5-fold cross validation was
226 repeated 10 times, each with a random split of the gold standard into training and test sets. The results of
227 the 5-fold cross validation showed excellent results, with an average area under the receiver operator
228 characteristic (AUROC) of 0.95 and average precision (AUPRC) of 0.74 (Figure 1A and 1B). These
229 results are consistent with a very accurate classifier, and comparable to results seen in similar
230 computational repositioning studies [6, 9, 11]. To further evaluate the accuracy of these predictions, the
231 prediction rankings of test set indications were examined for given drugs and diseases (Figure 1C and
232 1D). The median value for the rank of a positive disease, given a test-set positive drug was 18 out of 740
233 total diseases. Similarly, when examining the test-set positive diseases, the median rank for a positive
234 drug was 32 out of a possible 1330 examined compounds.

235 The ElasticNet logistic regression in this analysis used feature selection to reduce the risk of
236 overfitting with a highly complex model. In comparing the models, there was a fairly consistent selection
237 of short metapaths with only two edges that include important drug-drug or disease-disease similarity
238 measures (Figure 1E). These include two related drugs, one of which treats a disease
239 (dwpc_CDrtCDtDO), or two associated diseases, one of which has a known drug treatment
240 (dwpc_CDtDOawDO). However, other metapaths of length 3 which encapsulated drug-drug or disease-
241 disease similarities were also highly ranked. This includes two drugs that co-localize to a given
242 anatomical structure (dwpc_CDloAloCDtDO), two diseases that present in the same anatomical structure
243 (dwpc_CDtDOloAloDO), or diseases that affect similar phenomena (dwpc_CDtDOafPHafDO). In this
244 case anatomical structures could include body regions, organs, cell types or components, or tissues, while
245 phenomena include biological functions, processes, or environmental effects. It is important to again note
246 that these ‘similarity measures’ are purely derived from text-mined relations.

247 While these results indicate a fairly accurate classifier in this synthetic setting, the paradigm
248 under which they are trained and tested is not necessarily optimal for finding novel drug-disease

249 indications. A cross-validation framework essentially optimizes finding a subset of indication data that
250 has been *randomly* removed from a training set. However, prediction accuracy on randomly removed
251 indications does not necessarily extrapolate to prospective prediction of new drug repurposing candidates.
252 Framing the evaluation framework instead as one of future prediction based on past examples may be
253 more informative. For example, the question ‘given today’s state of biomedical knowledge, can future
254 indications be predicted?’ may more closely reflect the problem being addressed in drug repositioning.
255 The best way to address this question would be to perform the predictions in a time-resolved fashion,
256 training on contemporary data and then evaluating the model’s performance on an indication set from the
257 future.

258 **Building time-resolved networks**

259 To facilitate a time-resolved analysis, both the knowledge base data and the training data need to be
260 mapped to a particular time point. Each triple in SemMedDB is annotated with a PMID, indicating source
261 abstract of this text-mined data. Using the PMID, each triple, corresponding to an edge in the final
262 network, can be mapped to a specific date of publication. The DrugCentral database also includes
263 approval dates from several international medical agencies for the majority of the drugs. By filtering the
264 edges in the network by date, an approximate map of the biomedical knowledge of a given time period
265 can be produced. Therefore, we generated multiple networks, each representing distinct time-points. We
266 then applied the machine learning pipeline to each of these networks to evaluate the expected
267 performance on future drug-disease indications. Combining these sources of time-points for the network
268 serves to replicate the paradigm of training a machine learning model on the current state of biomedical
269 knowledge, evaluating its ability to predict what indications are likely to be found useful in the future.

270 Knowledge networks were built in a time-resolved fashion for each year, starting with 1950 and
271 continuing until the present. This was accomplished by removing edges with their earliest supporting
272 PMID dated after the desired year of the network. If either a drug or a disease from a known gold
273 standard indication was no longer connected to any other concept in the network, the indication was also
274 removed from the training and testing set for that network year. Examining the trends of the networks

275 constructed for the various timepoints, the number of nodes and edges always increased, but edges
276 increased more quickly with later timepoints producing a more connected network than earlier (Figures
277 2A and 2B).

278 The number of indications that could be mapped to a given network year increased quickly at first
279 but rose much more slowly in the later years of the network, even though the total number of concepts in
280 the network continued to increase. For the majority of the years of the network, the split between current
281 and future indications remained at a ratio of around 80% current and 20%, ideal for a training and testing
282 split. However, after the year 2000, the number of mappable future indications continued to diminish year
283 after year, reducing the test set size for these years (Supplemental Figure S2, Additional File 1).

284 **Machine learning results**

285 The performance of each model against a test set of future indications steadily increased from the earliest
286 time-point until the 1987 network. The AUROC metric saw continual increases over the entirety of the
287 network years, though these increases occurred more slowly after the 1987 network (Figure 3A). Looking
288 at average precision, this metric peaked at the 1987 timepoint with a value of 0.492, and then fell sharply
289 at 2000 and beyond, likely due to the diminished number of test-set positives. The AUROC of this peak
290 average precision time point of 1985 was 0.822. These peak performance metrics fall far below those
291 found via 5-fold cross-validation indicating an inherent limitation in evaluating models via this paradigm.

292 Similar to the cross-validation results, the models favored metapaths that represented drug-drug
293 and disease-disease similarity (Figure 3B). Specifically, the metapaths of type ‘Chemical & Drug -
294 TREATS - Disorder - ASSOCIATED WITH - Disorder’ (dwpc_CDtDOawDO) and ‘Chemical & Drug -
295 RELATED_TO - Chemical & Drug - TREATS - Disorder’ (dwpc_CDrtCDtDO) had the highest weights
296 across almost all models. One difference found from the cross-validation results is the appearance of the
297 ‘Physiology’ metanode in two of the top selected metapaths, one connecting two diseases through
298 common physiology, and one connecting two drugs that both augment a particular physiology. Model
299 complexity was also diminished compared to those seen in during cross-validation, with the majority of

300 models selecting less than 400 features, or 20% of the total available (Supplemental Figure S3, Additional
301 File 1).

302 Finally, one question to explore is whether or not there is a temporal dependence on the ability to
303 predict indications. For example, is there better performance on drugs approved 5 years into the future
304 rather than 20, since one only 5 years pre-approval may already be in the pipeline with some important
305 associations already known in the literature. To answer this, the results from all network years were
306 combined via z-scores. Grouping indications by approval relative to the year of the network allowed for
307 an AUROC metric to be determined for different timepoints into the future (Figure 3C). This analysis
308 revealed that there is still a substantial predictive ability for drugs approved up to about 5 years into the
309 future. However, after 5 years, this value quickly drops to a baseline of .70 for the AUROC and .15 for
310 the average precision. These results indicate a temporal dependence on the ability to predict future
311 indications, with the model being fairly inaccurate when looking far into the future.

312 **Edge dropout confirms importance of drug disease links**

313 Many other efforts in computational repositioning have found that emphasis on drug-drug and disease-
314 disease similarity metrics results in accurate predictors [6, 19, 20]. To further investigate the types of
315 information most impactful in improving the final model, an edge dropout analysis was run. The 1985
316 network was chosen as a base network for this analysis both due to its relatively strong performance on
317 future indications and its centralized time point among all the available networks. By taking each edge
318 type, randomly dropping out edge instances at rates of 25%, 50%, 75% and 100%, and comparing the
319 resulting models, the relative importance of each edge type within the model could be determined. The
320 edge that was found to have the largest impact on the resulting model was the ‘Chemicals & Drugs -
321 TREATS - Disorders’ edge, reducing the AUROC by .098 (Figure 4A). This result reinforces the idea
322 that drug-disease links, particularly those with a positive treatment association, are highly predictive in
323 repositioning studies. The drug-drug (‘Chemicals & Drugs - RELATED_TO - Chemicals & Drugs’) and
324 disease-disease (‘Disorders - ASSOCIATED_WITH - Disorders’) similarity edges were the next two
325 most impactful edges on the overall model, both showing decreases of .015 in the AUROC when

326 completely removed. Overall, however most edges showed very little reduction in AUROC, even at 100%
327 dropout rate. This could indicate a redundancy in important connections between drugs and diseases that
328 the model can continue to learn on even when partially removed.

329 **Time-resolved edge substitution confirms edge importance**

330 While dropout identifies the most important associations between concepts to this predictive model, this
331 does not necessarily confirm that more data of these types will improve the model's results. To simulate
332 this the impact of the assimilation of new knowledge of a specific type, an edge replacement analysis was
333 performed on the 1985 network. This process allowed for the examination of how accumulating new real-
334 world data of a given type might affect the model. By taking a specific edge type and replacing all the
335 edges of that type with those from the other network years from 1950 to 2015, the potential effect of
336 gathering more data of these specific types over time could be examined. Similar to the dropout analysis,
337 the target edge of 'Chemicals & Drugs - TREATS - Disorders' had the greatest effect on the model's
338 performance, showing an increase of .108 when replaced with the most current version of the edge
339 (Figure 4B). Similarly, the AUROC showed a large loss of .081 when replaced with values from 1950.
340 The drug-drug and disease-disease similarity edges also showed significant performance increases when
341 replaced with contemporary values, while decreasing performance in performance when replaced with
342 1950 values. While the three edges that produced the greatest decrease in performance during the dropout
343 analysis also had the biggest benefit when adding future edges, not all behaved in this manner. For
344 example, the edge 'Anatomy - LOCATION_OF - Chemicals & Drugs' showed the fourth largest
345 decreases in performance during edge dropout analysis. When using past versions of this edge type with
346 the 1985 network, the performance did have a measurable decrease in AUROC of .012, however current
347 versions of this edge type only improved the score by .002. Conversely, the edge 'Physiology - AFFECTS
348 - Disorders' showed little to no performance loss during the dropout analysis and indeed showed little
349 performance change when using past versions of the edge (Supplemental Figure S4, Additional File 1).
350 However, this edge showed substantial increase of .012 AUROC when using contemporary versions of
351 the edge. Finally, some edge types like 'Genes & Molecular Sequences - ASSOCIATED WITH -

352 Disorders' actually performed slightly better with past version or future versions of the edge, when
353 compared 1985 version of the edge, with an increase in AUROC of .004 with contemporary edges and an
354 increase of .011 with edges from 1950 (Supplemental Figure S5, Additional File 1). This further
355 underscores the idea that a time-resolved analysis provides a more complete picture of the important
356 components to a learning model.

357 **Discussion and Conclusions**

358 While a text-mined data source, SemMedDB performed very well when using the metapath-based
359 repositioning algorithm from Rephetio and trained and tested against a DrugCentral derived gold
360 standard. However, performing well in a cross-validation does not necessarily lead to a large number of
361 real-world repositioning candidates. This evaluation paradigm essentially trains the learning model to
362 identify indications that are currently known but simply withheld from a dataset. In the real world, the
363 problem solved by computational repositioning is more closely aligned to attempting to predict new
364 indications that are not already known at this current time-point. Our use of time-resolved knowledge
365 networks has allowed us to replicate this paradigm and expose a marked reduction in performance when a
366 model is tested in this fashion. Time separation is a long-used practice to combat overfitting in data
367 mining [21] and our application of this practice to compound repositioning may help explain some of the
368 discrepancy between model performance and the number of repositioning candidates successfully
369 produced through computational repositioning.

370 We believe that this method for evaluating a repositioning algorithm in a time-resolved fashion
371 may more accurately reflect its ability to find true repurposing candidates. Identifying algorithms that
372 perform well at predicting future indications on the time-resolved networks presented in this paper may
373 yield better results when translating retrospective computational analyses to the prospective hypothesis
374 generation. As these networks are built around text-mined data, predictive performance may be enhanced
375 by utilizing high-confidence, curated, data sources for computational repositioning. The original date of
376 discovery for a given data point has shown itself to be an important piece of metadata in evaluating a
377 predictive model. Ensuring curated data sources are supported by evidence that can be mapped back to an

378 initial date of discovery functions to enhance the utility of the data in predictive models such as these.

379 Finally, this temporal analysis again supports the notion that drug and disease similarity measures as well

380 as direct associations between these concepts are still the most important pieces of data in generating a

381 predictive model. Further enhancing our understanding of mechanistic relationships that these concepts

382 will likely result in further increases to computational repositioning performance.

383

384 **List of abbreviations**

385 Hetnet – heterogeneous network, NLP – Natural Language Processing, SemMedDB – Semantic Medline

386 Database, PMID – PubMed Identifier, DWPC – Degree Weighted Path Count, AUROC – Area Under the

387 Receiver Operator Curve, AUPRC – Area Under the Precision Recall Curve (aka average precision),

388 UMLS – Unified Medical Language System, MeSH – Medical Subject Headings

389 **Ethics approval and consent to participate**

390 Not applicable.

391 **Consent for publication**

392 Not applicable.

393 **Availability of data and materials**

394 Data for SemMedDB hetnet building: The SemMedDB database used to build the heterogeneous network

395 analyzed in this study are available here: <https://skr3.nlm.nih.gov/SemMedDB/index.html>

396 The UMLS Metathesaurus used for identifier cross-referencing are available

397 <https://www.nlm.nih.gov/research/umls/licensedcontent/umlsknowledgesources.html>

398 These data are provided by the UMLS Terminology Service, but restrictions apply to the availability of

399 this data, which were used under the UMLS Metathesaurus License.

400 https://www.nlm.nih.gov/databases/umls.html#license_request ^[14]

401 Data for gold standard: The DrugCentral database used to build the gold standard for this study is freely

402 available from DrugCentral under the CC-BY-SA-4.0 license. <http://drugcentral.org/> ^[15]

403 Source code to download the above datasets and reproduce the analysis found in this current study is
404 available on GitHub in the following repository. <https://github.com/mmayers12/semmed>

405 **Competing interests**

406 The authors declare they have no competing interests.

407 **Funding**

408 This work was funded by NIH grants OT3TR002019 and R01GM089820.

409 **Author's contributions**

410 MM developed the network building pipeline, adapted the machine learning algorithm for use with
411 SemMedDB, and wrote the majority of the manuscript. TL developed the DrugCentral gold standard and
412 designed the feature performance analysis experiments. NQ organized graph data and participated in
413 design of the experiments. The research was performed under the advice and supervision of AS. All
414 authors read and approved the final manuscript.

415 **Acknowledgements**

416 N/A

417 **Additional files**

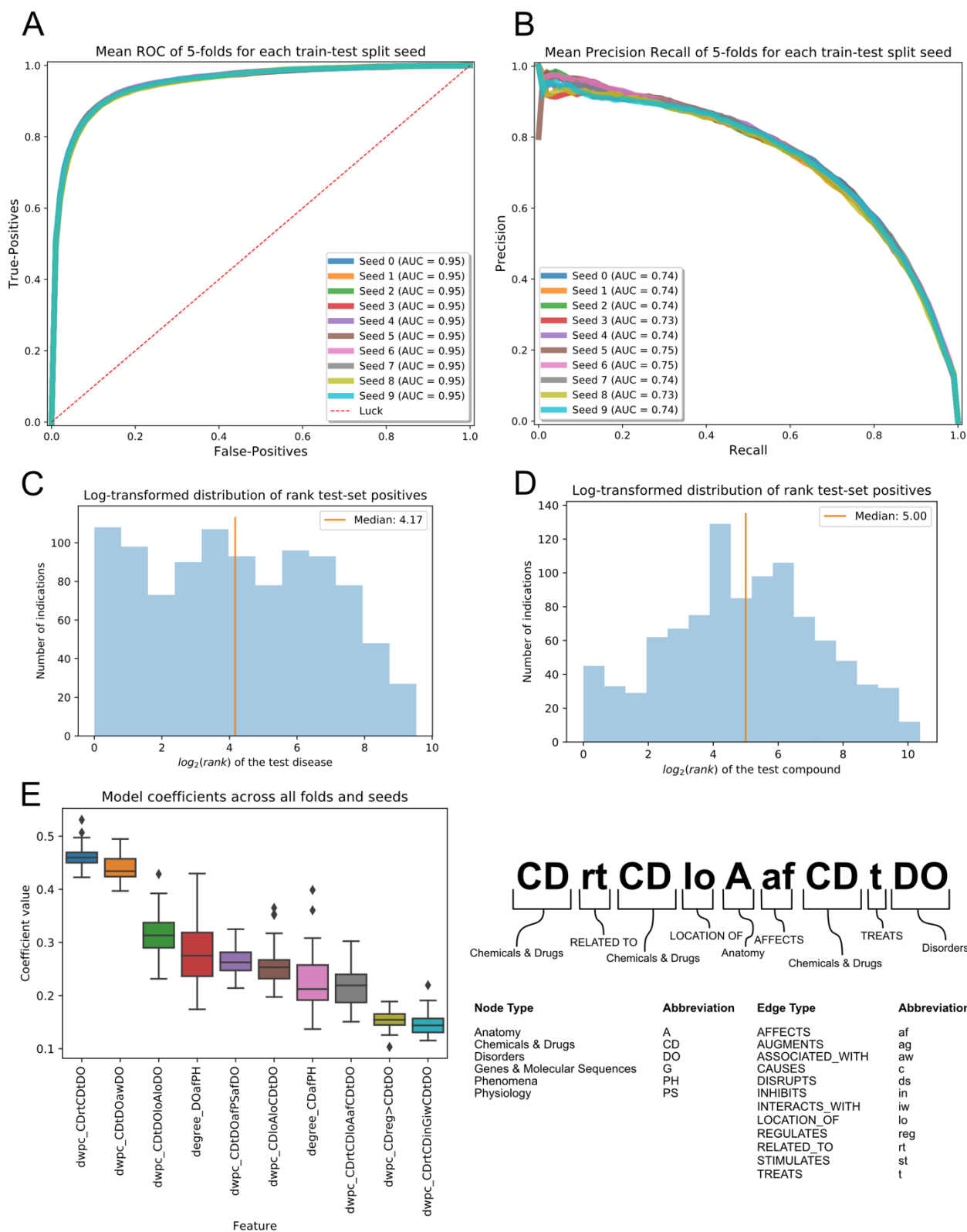
418 Additional File 1: Supplemental Figures

419 **References**

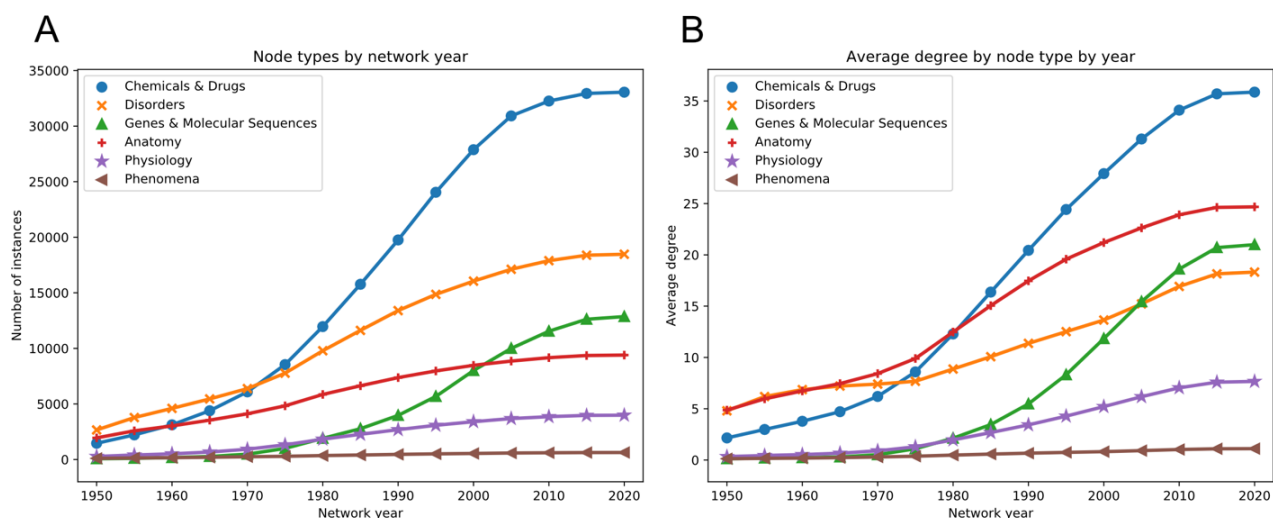
- 420 1. Ashburn TT, Thor KB. Drug repositioning: identifying and developing new uses for existing drugs. *Nat*
421 *Rev Drug Discov.* 2004;3:673–83.
- 422 2. Li J, Zheng S, Chen B, Butte AJ, Swamidass SJ, Lu Z. A survey of current trends in computational
423 drug repositioning. *Brief Bioinform.* 2016;17:2–12.
- 424 3. Yella J, Yaddanapudi S, Wang Y, Jegga A, Yella JK, Yaddanapudi S, et al. Changing Trends in
425 Computational Drug Repositioning. *Pharmaceuticals.* 2018;11:57.
- 426 4. Sirota M, Dudley JT, Kim J, Chiang AP, Morgan AA, Sweet-Cordero A, et al. Discovery and
427 Preclinical Validation of Drug Indications Using Compendia of Public Gene Expression Data. *Science*
428 *Translational Medicine.* 2011;3:96ra77-96ra77.

- 429 5. Issa NT, Kruger J, Wathieu H, Raja R, Byers SW, Dakshanamurthy S. DrugGenEx-Net: a novel
430 computational platform for systems pharmacology and gene expression-based drug repurposing. BMC
431 Bioinformatics. 2016;17:202.
- 432 6. Gottlieb A, Stein GY, Ruppin E, Sharan R. PREDICT: a method for inferring novel drug indications
433 with application to personalized medicine. Molecular Systems Biology. 2011;7:496.
- 434 7. Chen H, Zhang H, Zhang Z, Cao Y, Tang W. Network-Based Inference Methods for Drug
435 Repositioning. Computational and Mathematical Methods in Medicine. 2015. doi:10.1155/2015/130620.
- 436 8. Cheng F, Liu C, Jiang J, Lu W, Li W, Liu G, et al. Prediction of Drug-Target Interactions and Drug
437 Repositioning via Network-Based Inference. PLOS Comput Biol. 2012;8:e1002503.
- 438 9. Luo H, Wang J, Li M, Luo J, Peng X, Wu F-X, et al. Drug repositioning based on comprehensive
439 similarity measures and Bi-Random walk algorithm. Bioinformatics. 2016;32:2664–71.
- 440 10. Oprea TI, Overington JP. Computational and Practical Aspects of Drug Repositioning. Assay Drug
441 Dev Technol. 2015;13:299–306.
- 442 11. Himmelstein DS, Lizee A, Hessler C, Brueggeman L, Chen SL, Hadley D, et al. Systematic
443 integration of biomedical knowledge prioritizes drugs for repurposing. eLife Sciences. 2017;6:e26726.
- 444 12. Gonzalez GH, Tahsin T, Goodale BC, Greene AC, Greene CS. Recent Advances and Emerging
445 Applications in Text and Data Mining for Biomedical Discovery. Brief Bioinform. 2016;17:33–42.
- 446 13. Rindflesch TC, Fiszman M. The interaction of domain knowledge and linguistic structure in natural
447 language processing: interpreting hypernymic propositions in biomedical text. Journal of Biomedical
448 Informatics. 2003;36:462–77.
- 449 14. Kilicoglu H, Shin D, Fiszman M, Rosembat G, Rindflesch TC. SemMedDB: a PubMed-scale
450 repository of biomedical semantic predications. Bioinformatics. 2012;28:3158–60.
- 451 15. Ursu O, Holmes J, Knockel J, Bologna CG, Yang JJ, Mathias SL, et al. DrugCentral: online drug
452 compendium. Nucleic Acids Res. 2017;45 Database issue:D932–9.

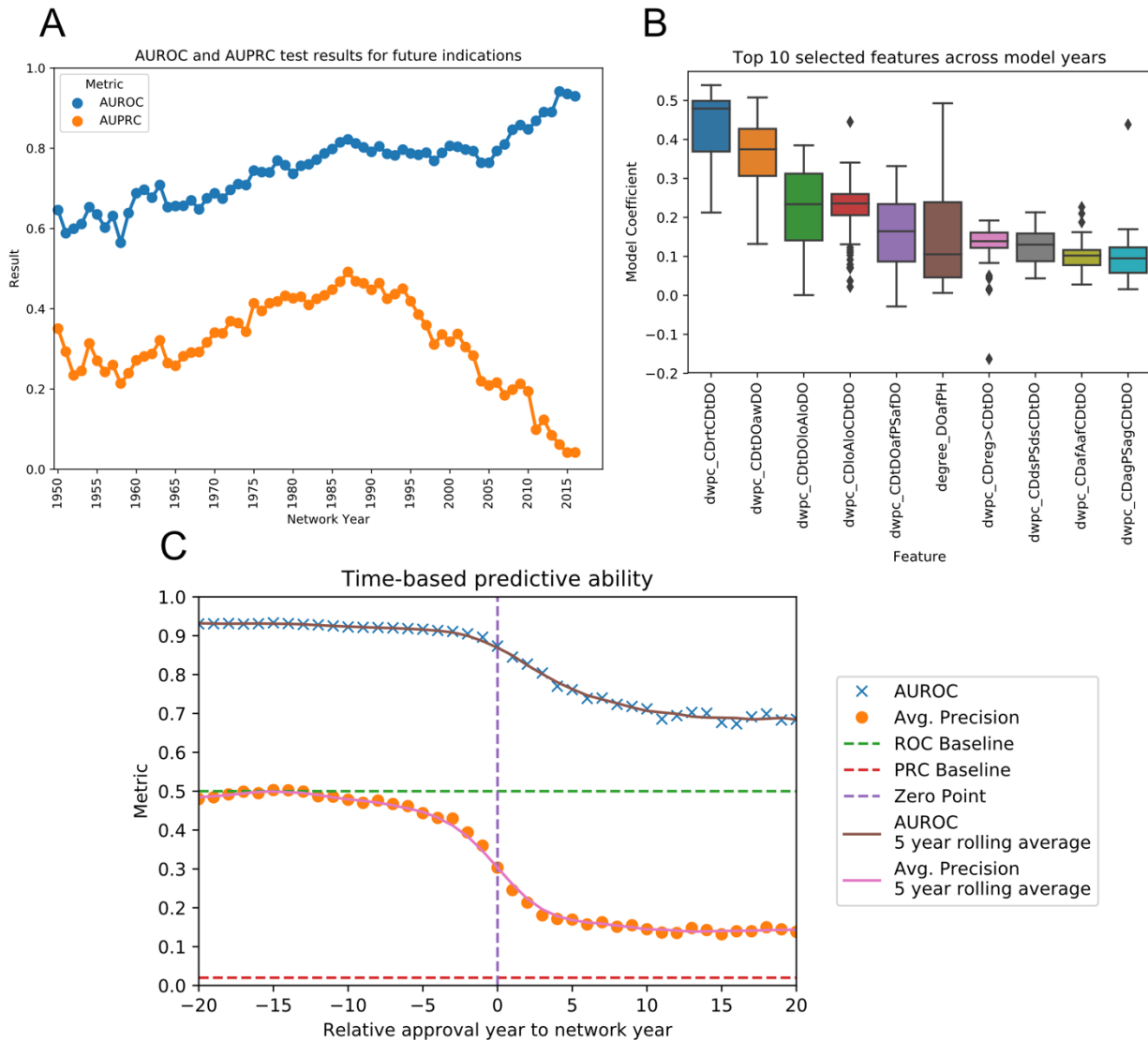
- 453 16. Sun Y, Barber R, Gupta M, Aggarwal CC, Han J. Co-author Relationship Prediction in
454 Heterogeneous Bibliographic Networks. In: 2011 International Conference on Advances in Social
455 Networks Analysis and Mining. 2011. p. 121–8.
- 456 17. Himmelstein DS, Baranzini SE. Heterogeneous Network Edge Prediction: A Data Integration
457 Approach to Prioritize Disease-Associated Genes. *PLOS Computational Biology*. 2015;11:e1004259.
- 458 18. Friedman J, Hastie T, Tibshirani R. Regularization Paths for Generalized Linear Models via
459 Coordinate Descent | Friedman | Journal of Statistical Software. *Journal of Statistical Software*. 2010;33.
460 doi:10.18637/jss.v033.i01.
- 461 19. Lu L, Yu H. DR2DI: a powerful computational tool for predicting novel drug-disease associations.
462 *Journal of Computer-Aided Molecular Design*. 2018;5:633–42.
- 463 20. Luo H, Li M, Wang S, Liu Q, Li Y, Wang J, et al. Computational drug repositioning using low-rank
464 matrix approximation and randomized algorithms. *Bioinformatics*. 2018;34:1904–12.
- 465 21. Kaufman S, Rosset S, Perlich C. Leakage in Data Mining: Formulation, Detection, and Avoidance. In:
466 Proceedings of the 17th ACM SIGKDD International Conference on Knowledge Discovery and Data
467 Mining. New York, NY, USA: ACM; 2011. p. 556–563. doi:10.1145/2020408.2020496.
- 468



470 **Figure 1:** 5-fold cross validation results for SemMedDB network using DrugCentral gold standard. **A)**
471 Receiver-Operator Characteristic curve displaying the mean result across 5-folds. Ten different seed
472 values for randomly splitting indications in 5 are compared showing very little variation. **B)** Precision-
473 Recall curve for the mean result across 5-folds, with ten different split seeds displayed. **C)** Histogram of
474 \log_2 transformed rank of true positive disease for a given test-set positive drug, taken from a
475 representative fold and seed of the cross-validation. If a drug treats multiple diseases, the ranks of all
476 diseases treated in the test-set indications are shown. **D)** Histogram of \log_2 transformed rank of true
477 positive drug for a given test-set disease, chosen from same fold and seed as C. If a disease is treated by
478 multiple drugs in the test-set indications, all ranks are included. **E)** (left) Boxplot of 10 largest model
479 coefficients in selected features across all folds and seeds. (right) Breakdown of metapath abbreviations.
480 Node abbreviations appear in capital letters while edge abbreviations appear lower case.
481



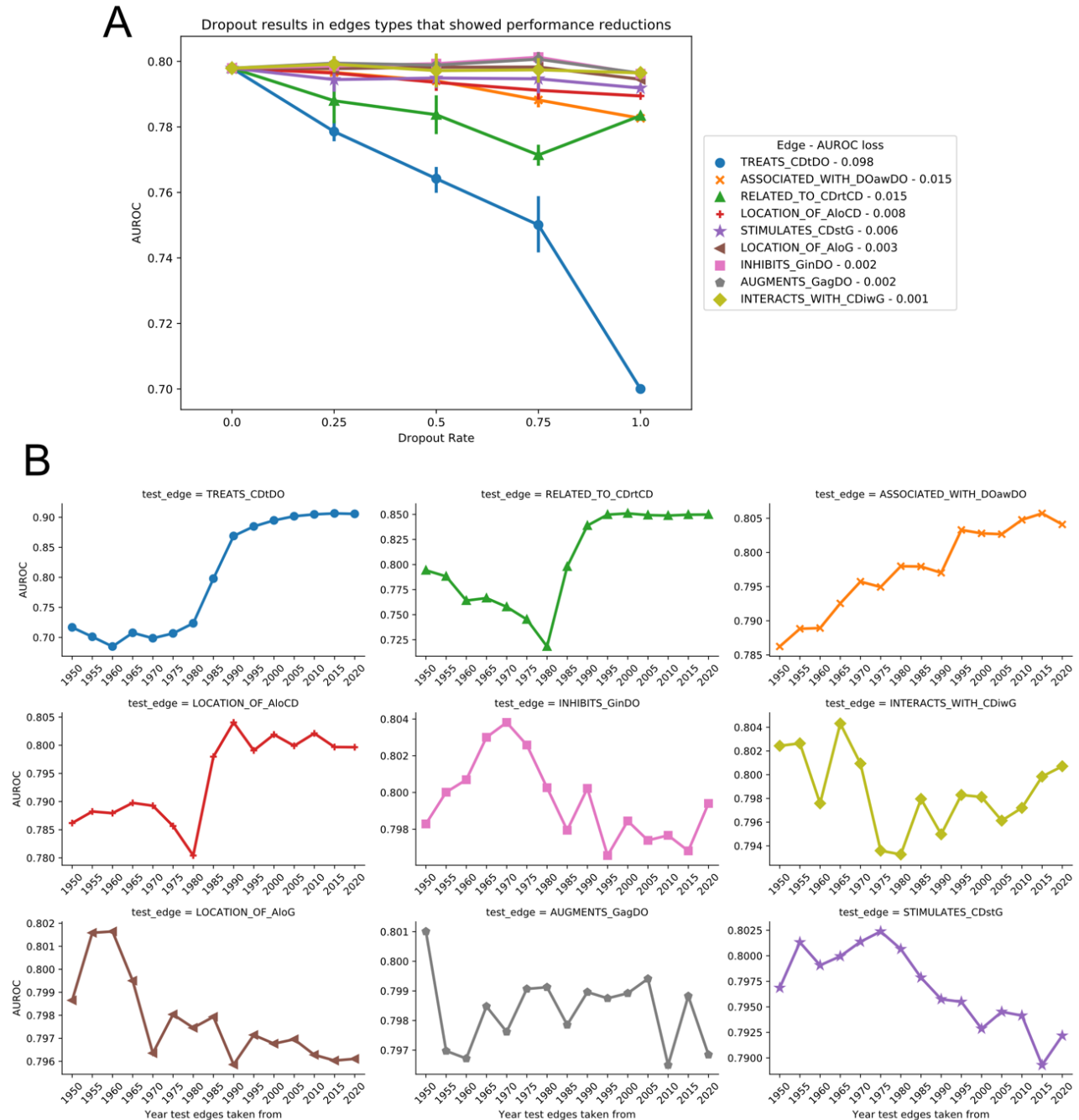
482 **Figure 2:** Time-resolved network build results. **A)** Number of nodes of a given type by network year. **B)**
483 Average node degree for each node type across all network years.
484
485



486

487 **Figure 3:** Machine learning results for the time-resolved networks. **A)** Performance metrics for the test-
 488 set (future) indications across the different network years. Only drugs approved after the year of the
 489 network are included in the test-set, while those approved prior are used for training. **B)** Box plots of the
 490 values of the model coefficients across all of the different network years. The top-10 coefficients with
 491 largest mean value across all models are shown. **C)** AUROC and AUPRC data for indications based on
 492 their probabilities, split by the number of years between drug approval date and the year of the network.

493 Values to the left of the Zero Point are indications approved before the network year thus part of the
 494 training-set, while those to the right are part of the test-set. Probabilities for all drug-disease pairs were
 495 standardized before combining across models. Points are given for each data point, while lines represent a
 496 5-year rolling average of metrics.
 497



499 **Figure 4:** Analysis of edge type importance to the overall model. **A)** Edge dropout analysis showing the
500 reduction in AUROC metric when the edges are dropped out at rates of 25, 50, 75, and 100%. Error bars
501 indicate 95% confidence interval over 5 replicates with different seeds for dropout. The 9 edge types that
502 had the greatest reduction from 0 to 100% dropout are displayed. **B)** Edge replacement analysis showing
503 changes in AUROC when edges are replaced with those of the same type from another year's network.
504 The top 9 edges that showed greatest loss in performance in the dropout analysis between 0 and 100%
505 dropout are displayed.
506